Controlled Protein Embedment onto Au/Ag Core−Shell Nanoparticles for Immuno-Labeling of Nanosilver Surface

In Hwan Lee, Jeong Min Lee, and Yongwon Jung*

Department of Chemistry, Korea Advanced Institute of Science and Technology, Daejeon 305-701, Korea

Ⓢ *Supporting Information*

ABSTRACT: Difficulties in stable conjugation of biomolecules to nanosilver surfaces have severely limited the use of silver nanostructures in biological applications. Here, we report a facile antibody conjugation onto gold/silver (Au/Ag) core−shell nanoparticles by stable and uniform embedment of an antibody binding protein, protein G, in silver nanoshells. A rigid helical peptide linker with a terminal cysteine residue was fused to protein G. A mixture of the peptide-fused protein G and space-filling free peptide was reacted with gold nanoparticles (AuNPs) to form a protein G-linked peptide layer on the particle surface. Uniform silver nanoshells were successfully formed on these protein G-AuNPs, while stably embedding protein G-linked peptide layers. Protein G specifically targets the Fc region of an antibody and thus affords properly oriented antibodies on the particle surface. Compared to Au nanoparticles of similar size with randomly adsorbed antibodies, the present immuno-labeled Au/Ag core−shell nanoparticles offered nearly 10-fold higher sensitivities for naked-eye detection of surface bound antigens. In addition, small dye molecules that were bonded to the peptide layer on Au nanoparticles exhibited highly enhanced surface-enhanced Raman scattering (SERS) signals upon Ag shell formation. The present strategy provides a simple but efficient way to conjugate antibodies to nanosilver surfaces, which will greatly facilitate wider use of the superior optical properties of silver nanostructures in biological applications.

KEYWORDS: *nanosilver surface, Au/Ag core−shell NPs, protein embedment, immuno-labeling, orientation, SERS*
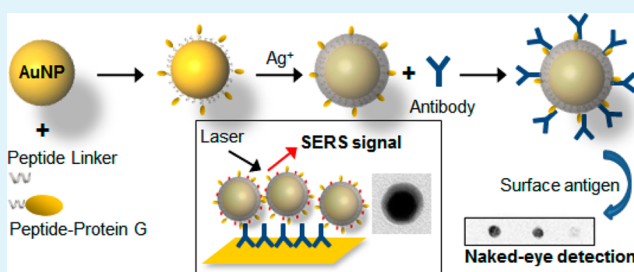
1. INTRODUCTION

Offering distinct optical and electrochemical properties, gold (Au) and silver (Ag) nanoparticles (and their hybrid structures) have been widely used in numerous biomedical and bioanalytical applications.[1−6] Various biomolecules such as antibodies and nucleic acids are conjugated to the particle surfaces in these applications.[7−10] Ideally, bioconjugated nanostructures would feature stably-maintained bio-functionality, well-defined surfaces, low nonspecific binding background (selectivity), and stability in the required buffer mediums. At present, Au nanoparticles (AuNPs) are predominantly used for biological applications over AgNPs, mainly due to their ability to form stably-functionalized bioconjugates via simple chemistry.[3]

AgNPs are a technologically important material. Most notably, they offer the highest conductivity and reflectivity among all metals and exhibit size-dependent catalytic activity.[11,12] The extinction coefficient of AgNPs is significantly higher (up to four times) than that of AuNPs of similar size, and Ag nanostructures have proven to be highly valuable for various colorimetric/optical detections.[13−15] In addition, Raman scattering and fluorescence signals are significantly enhanced on the surfaces of various silver nanostructures, which can serve as highly sensitive optical sensing probes.[16,17] Surface-enhanced Raman scattering (SERS) on dimeric Au/Ag core−shell nanoparticles recently has been well characterized on a single molecule level.[18,19] In general, Ag provides significantly higher Raman enhancement factors and also a wider range of suitable excitation wavelengths for SERS than Au.[20,21]

Despite these advantages, AgNPs are sensitive to the surrounding chemicals, leading to easy oxidization and degradation of their plasmonic properties. Furthermore, the preparation of bio-functionalized AgNPs (such as antibody conjugates) that remain stable in physiological buffers has proven difficult.[22] AgNPs often require additional coatings to passivate and/or conjugate the nanoparticles to target antibodies.[23,24] Synthetic multi-thiol linkers were also applied to fabricate stable DNA-AgNP conjugates.[25] To fully exploit the advantages of AgNPs as distinctive labeling probes, improved preparation strategies for stable and uniform protein conjugation to the nanosilver surfaces are required.

Here, we describe a facile method for oriented antibody immobilization on silver surfaces of Au/Ag core−shell NPs via antibody binding protein (Protein G), which is first stably conjugated to bare AuNPs and embedded into the Ag shells upon Ag deposition on AuNP-protein G conjugates. Uniform surface modification of AuNPs is critical for Ag shell formation

and biomolecule embedment, as previously reported with DNA-embedded Au/Ag NPs.[26] However, general protein adsorption onto an AuNP surface is highly heterogeneous. Here, we genetically introduced a rigid peptide linker with a cysteine residue to protein G. This peptide-fused protein G and a synthetic free peptide linker formed a uniform and densely packed peptide layer on AuNPs. Ag shell formation with embedded protein G and subsequent antibody conjugation were confirmed with transmission electron microscopy (TEM), absorbance spectroscopy, and gel electrophoresis analyses. Captured antibodies were well arranged and fully retained their binding abilities on Au/Ag hybrid structures. The immuno-labeled core−shell NPs were specifically addressed to target antigens such as PSA and IL6 proteins on membrane surfaces with highly improved sensitivities compared to antibody-adsorbed AuNPs. Our protein embedded silver shells also provided highly efficient and uniform nano-surfaces for SERS of various small molecules.

2. EXPERIMENTAL SECTION

Materials. Bovine serum albumin (BSA) and human immunoglobulin G (hIgG) were purchased from Sigma. Anti-human kallikrein 3/PSA, anti IL6 antibody, and antigens (PSA and IL6) were purchased from R&D Systems. The peptides with the following sequences were obtained from PEPTRON: CA(EAAAK)$_3$A and CA(EAAAK)$_3$AK-TAMRA (carboxytetramethylrhodamine). Gold and silver nanoparticles (15 and 20 nm) were purchased from BBInternational. Silver staining solution B (hydroquinone solution), AgNO$_3$, and Rhodamine B isothiocyanate were also purchased from Sigma. Helical peptide fused protein G (Peptide-Protein G in Figure 1) was
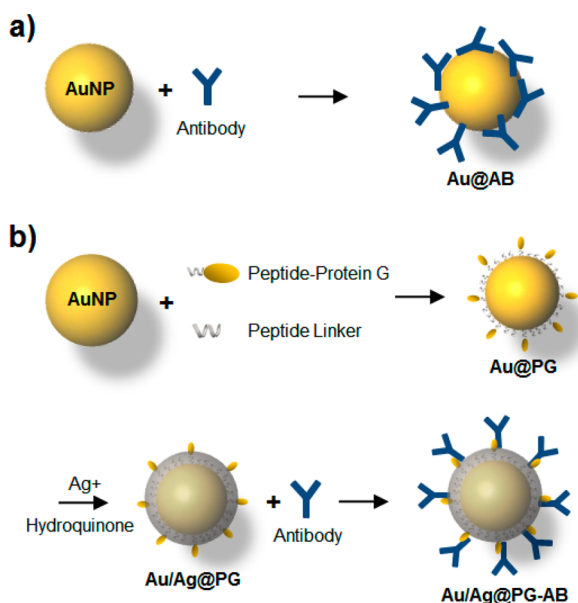

Figure 1. Schematic representations of the preparation of (a) antibody-conjugated AuNPs via random adsorption (Au@AB) and (b) antibody-conjugated Au/Ag core−shell NPs via embedded protein G (Au/Ag@PG-AB).

constructed by introducing CA(EAAAK)$_3$A amino acids to the N-terminus of a single antibody binding domain (B2 domain) of protein G (sequence in Supporting Information (SI) Figure S1). Recombinant protein was expressed and purified by following the previously reported method.[27]

Preparation of Au and Ag NP Conjugates. To prepare the antibody-conjugated AuNPs (Au@AB in Figure 1a) and AgNPs (Ag@AB) via conventional random adsorption, 10 μL of antibody solution

(1 mg/mL in PBS) was added to 500 μL of 1 nM NP colloid (20 nm in diameter) solutions. Borate buffer (pH 8.5) was then added to the mixture for a 10 mM final concentration. Following incubation for 30 min at room temperature with constant mixing, BSA (1 mg/mL final concentration) was added to the solution to block the AuNP and AgNP surfaces. After incubation for 15 min at room temperature, the mixture was centrifuged at 10 000 rpm at 4 °C for 20 min. The supernatant was discarded, and the resulting AuNP and AgNP conjugates were resuspended in 10 mM sodiumbicarbonate buffer.

Protein G conjugated AuNPs (Au@PG in Figure 1b) were prepared by adding a mixture of a synthetic Peptide Linker (10 μM) and Peptide−Protein G (1 μM) to 3 nM citrate stabilized 15 nm AuNPs (500 μL). To uniformly introduce Raman dye (TAMRA) to the AuNPs, Peptide Linker−TAMRA (5 μM) was also applied to the NPs with Peptide Linker (5 μM) and Peptide−Protein G (1 μM). After 20 min incubation with constant shaking, 5 μL of 10% SDS solution (NANOpure water, 18.2 MΩ) was added to the mixture. This final mixture was again gently shaken for overnight. The resulting conjugates were separated from excess unbound peptides and proteins by centrifugation and resuspended in 10 mM sodiumbicarbonate buffer.

Silver Shell Formation. 1 mM AgNO$_3$ was added to 500 μL of 1 nM Au@PG to produce various concentrations (100 nM, 200 nM, and 500 nM), and 2 μL of diluted hydroquinone solution (1/10 dilution from commercial silver enhancing solution) was rapidly added to the solutions. The mixtures were vigorously mixed and incubated at room temperature. Silver deposition on protein-bound AuNP surfaces reached equilibrium within 1 h, inducing a red wine to orange color change. These protein G-embedded Au/Ag core−shell NPs (Au/Ag@PG) were washed with centrifugation and resuspended with 10 mM sodiumbicarbonate buffer with 1 mg/mL BSA. Antibodies (100 nM final concentration) were simply added to Au/Ag@PG to form immuno-labeled Au/Ag core−shell NPs (Au/Ag@PG-AB). The resulting antibody-NP conjugates were analyzed on 1.2 % agarose gels with 0.5 X TAE (10 mM acetic acid, 0.5 mM EDTA, and 20 mM Tris pH 8.0) as a running buffer and were also characterized by SDS-PAGE.

Field-Emission Transmission Electron Microscopy (FE-TEM). The fabricated NP conjugates were visualized with a FE-TEM (JEM-2100F(HR), JEOL Ltd.). NP solutions were adsorbed onto a carbon-coated copper grid (200 mesh) and air-dried for 2 min. To analyze conjugated proteins on NPs, the NP conjugates were examined with a FE-TEM after negative staining with 2% uranyl acetate (Electron Microscopy Sciences) for 30 s. Energy dispersive spectroscopy (EDS) of the NP conjugates was also performed in this configuration.

In Vitro Binding Experiments. Varying amounts of antigens, PSA and IL6 (1 μg, 100 ng, 10 ng), were spotted on an NC membrane. After 10 min incubation, the protein spotted membranes were submerged into Blocking Solution (1 mg/mL BSA in PBS) for 1 h. Membranes were rinsed with PBS several times and treated with various antibody conjugated NPs (1 nM). The present immuno-labeled Au/Ag core−shell NPs (Au/Ag@PG-AB) were compared with conventional antibody-adsorbed AuNPs (Au@AB). A silver shell was also formed on Au@AB, which produced highly unstable Au/Ag@AB. Au/Ag core−shell NPs without embedded protein G (Au/Ag@peptide) were also examined as a negative control. The autometallographic signals were developed for 1 h at room temperature with gentle shaking.

SERS Measurements. Protein G conjugated AuNPs and Au/Ag core−shell NPs were investigated as SERS active substrates to detect SERS signals from TAMRA molecules. A gold chip was incubated with human antibody (0.1 mg/mL) for 1 h to form an antibody layer on the gold surface. The antibody treated gold chips were rinsed with PBS and blocked with 1 mg/mL BSA solution. TAMRA and protein G conjugated AuNPs (1 nM) with (Au/Ag@PG) or without (Au@PG) silver shells were addressed to the antibody covered gold surface, and unbound NPs were removed by PBS washes. TMARA conjugated free peptide was also deposited and dried on the gold chip. Raman spectra were obtained with 512 nm excitation laser (Horiba Jobin Yvon, France) in Renishaw continuous mode with accumulation times of 10

s. The laser beam was focused on the sample in backscattering geometry using a 100× objective lens. To perform SERS measurements of randomly deposited Rhodamine B (Rh-B), protein G conjugated AuNPs (Au@PG) and Au/Ag core−shell NPs (Au/Ag@PG) were addressed to the antibody-covered gold surface as described above. The nanoparticle addressed gold surface was treated with 0.1 mM Rh-B in PBS, and the chips were dried at room temperature before SERS measurement.

3. RESULTS AND DISCUSSION

Gold nanoparticles (AuNPs) can be readily modified with ligands containing various functional groups, which can effectively recruit an array of biomolecules. Even simple adsorption is highly effective, and antibody-adsorbed AuNPs have been widely used for various immuoassays (Figure 1a). However, as discussed above, placing proteins such as antibodies on AgNP surfaces has been highly problematic. Au/Ag core−shell NP structures feature chemical versatilities of Au and strong optical properties of Ag. Previously, Au/Ag core−shell NPs were stably functionalized with DNA molecules that were embedded into Ag shells instead of being linked directly to Ag surfaces.[18,26] Synthetic DNAs were conjugated to AuNPs with a uniform density, and Ag shells were formed directly on these DNA-AuNPs. Uniform surface conjugation of proteins (particularly large ones such as antibodies) to AuNPs is, however, a highly challenging task. Indeed, chemical silver deposition on antibody-adsorbed AuNPs (Au@AB in Figure 1a) resulted in irregular shapes of Au/Ag structures and caused a high degree of aggregation (SI Figure S2), likely due to the highly heterogeneous AuNP surfaces.

We utilized a highly versatile antibody binding protein, protein G, for protein embedment into Au/Ag core−shell NPs and subsequent antibody conjugation. Protein G specifically targets the Fc region of an antibody and captured antibodies fully retain their binding abilities.[28] To minimize heterogeneity of protein-bound Au surfaces, a rigid peptide linker with a terminal cysteine residue [CA(EAAAK)$_3$A] was introduced (Peptide Linker in Figure 1b). The A(EAAAK)nA ($n \leq 6$) peptide is reported to form a helical structure and is generally used for distance control between fused proteins via this helical linear peptide.[29,30] The rigid and thiol-functionalized Peptide Linker was also fused to the N-terminal of protein G (Peptide−Protein G in Figure 1b). A mixture of Peptide Linker and Peptide−Protein G in a 10:1 ratio was reacted with citrate-stabilized 15 nm AuNPs in the presence of 0.1% SDS. The linearly structured peptide with a terminal thiol can form a uniform peptide layer on an AuNP surface. This provides high uniformity for Ag shell formation and optimal orientation/space for antibody capture by protein G. The Peptide Linker and Peptide−Protein G ratio can be varied to control the protein G densities on AuNPs. A high level display of protein G on AuNPs, however, caused inconsistent aggregation in buffer solutions. Au@PG constructed with an optimized Peptide Linker/Peptide−Protein G mixture (10:1) maintained nearly maximum antibody immobilization on the surface without any aggregation. Protein G-conjugated AuNPs (Au@PG) were directly reacted with commercially available silver staining solutions to form protein G-embedded Au/Ag core−shell NPs (Au/Ag@PG). The constructed NPs were stable in various buffered aqueous solutions and easily purified by simple centrifugation.

The fabricated NPs were visualized with a Field Emission Transmission Electron Microscope (FE-TEM). A Protein G-

linked peptide layer on AuNP appeared as a dark corona uniformly surrounding the nanoparticle, as observed after negative staining with 2% uranyl acetate (Au@PG in Figure 2a). A uniform protein G layer on the AuNP surface allowed
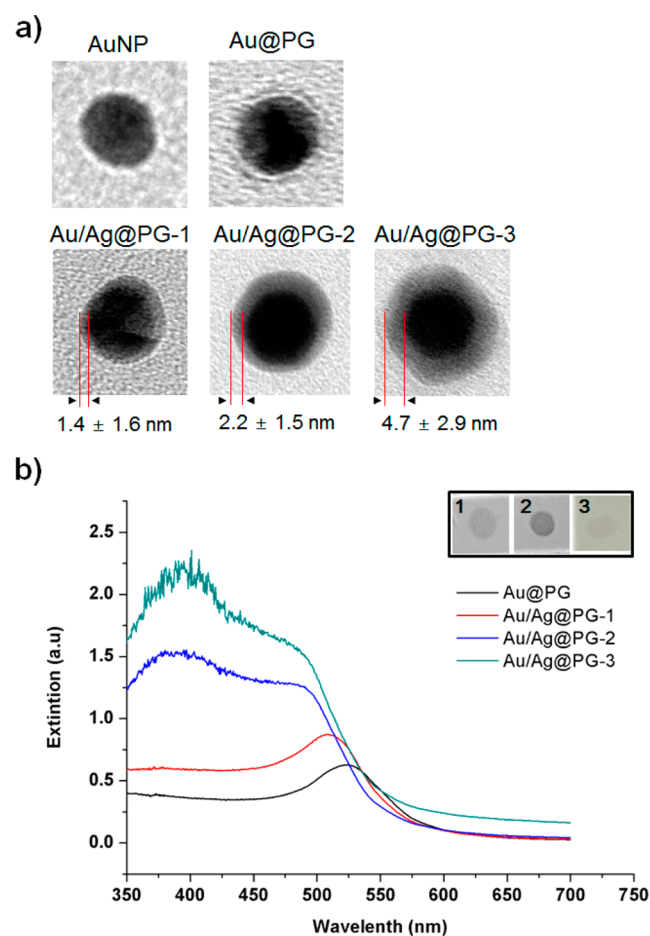

Figure 2. Characterization of Ag shell formation on protein-conjugated AuNPs. (a) TEM images of a bare gold nanoparticle (AuNP), protein G-covered AuNP (Au@PG), and protein G-embedded Au/Ag core−shell NPs with varying degrees of Ag shell formation (Au/Ag@PG-1, -2, -3). Au@PG was negatively stained to visualize bound proteins. (b) UV−visible absorption spectra for fabricated NPs. Protein G-embedded Au/Ag@PG-1, -2, and -3 NPs were reacted with membrane bound antibody spots (inset).

uniform Ag shell formation on the AuNP, as shown in TEM images of protein G-embedded Au/Ag core−shell NPs (Au/Ag@PG in Figure 2a). As previously reported,[26] an electron density image of the Au core was darker than that of the Ag shell. Varying concentrations of AgNO$_3$ were added for shell formation. With increased Ag ions from 100 nM and 200 nM to 500 nM, the thickness of the deposited silver shell also increased, from 1.4 ± 1.3 nm (Au/Ag@PG-1) and 2.2 ± 1.5 nm (Au/Ag@PG-2) to 4.7 ± 2.9 nm (Au/Ag@PG-3), respectively. A high degree of Ag deposition (Au/Ag@PG-3), however, often resulted in irregular oval shapes of Au/Ag core−shell NPs (data not shown). In addition, single-particle X-ray energy dispersive spectroscopy (EDS) analysis of Au/Ag@PG-1 and -2 showed an increased silver content as the Ag thickness increases (SI Figure S3).

The silver nanoshell formation was also monitored by UV−vis spectroscopy (Figure 2b). Upon Ag shell formation, the

7661

dx.doi.org/10.1021/am500960b | ACS Appl. Mater. Interfaces 2014, 6, 7659−7664

AuNP adsorption peak at 520 nm was shifted to 500 nm. As the Ag shell became thicker, a broad shoulder peak at around 400 nm (indicative of Ag shells) increased. Antibody binding abilities of fabricated Au/Ag@PG NPs were investigated by reaction with surface-bound antibodies on an NC membrane (Figure 2b, inset). Strong colors of Au/Ag@PG NPs allowed direct naked-eye observation of particle targeting to the antibody spots. The highest colorimetric signal was obtained from Au/Ag@PG-2, which contains ∼2.2 nm Ag shells. Compared to Au/Ag@PG-1 (∼1.4 nm Ag shell), Au/Ag@PG-2 clearly shows a more distinct absorption pattern of Ag shells, which offered stronger colorimetic signals. In the case of Au/Ag@PG-3, protein G may be buried by Ag shells with irregular shapes and a nearly 5 nm diameter, resulting in inefficient antibody targeting (Figure 2b). The estimated lengths of the linear helical Peptide Linker and protein G domain are ∼2.5 nm and ∼3 nm, respectively. Collectively, Au/Ag@PG-2 shows strong optical properties of Ag shells as well as an optimized shell thickness for protein embedment without disturbing protein G-antibody interaction. Au/Ag@PG-2 is also well dispersed in aqueous buffers (SI Figure S4) with a narrow size distribution, and was thereby selected for subsequent studies for immuno-labeling of Au/Ag core−shell NPs. However, the protein orientation and the embedded portion of Peptide-Protein G on Au/Ag chore shell NPs are still not clearly verified.

Fabrication steps of protein G-embedded Au/Ag core−shell NPs and subsequent antibody conjugation were monitored by agarose gel electrophoresis (Figure 3a). Narrow migration
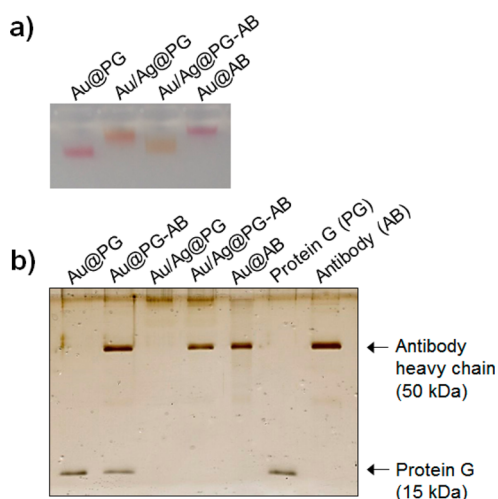

Figure 3. Gel electrophoretic analyses of antibody conjugated nanoparticles. (a) Agarose gel analysis of protein G-covered AuNPs (Au@PG), protein G-embedded Au@PG (Au/Ab@PG), antibody-conjugated Au/Ag core−shell NPs (Au/Ag@PG-AB), and antibody adsorbed AuNPs (Au@AB). (b) 15% SDS-PAGE analysis of NP surface-bound proteins. Protein G and IL-6 antibody lanes are indicated.

bands of the NP conjugates indicate a monodisperse nature of the particles.[27] Ag shell formation on Au@PG yielded a shifted

(and also narrow) band and color change (from red to orange) for the resulting Au/Ag@PG. Subsequent antibody (against IL-6) binding to Au/Ag@PG by simple addition of antibodies also resulted in shifted gel migration of Au/Ag@PG-AB (Figure 3a). Size changes of the nanoparticles covered with different proteins and Ag shells were also measured with direct light scattering (DLS) (Table 1 and SI Figure S5). Surface-bound protein G and antibodies were examined by sodium dodecyl sulfate polyacrylamide gel electrophoresis (SDS-PAGE) (Figure 3b). Proteins were released from the particle surfaces by boiling. IL-6 specific antibodies (mainly heavy chains were observed) were clearly bound to Protein G-embedded Au/Ag@PG. The protein G band, however, disappeared upon Ag shell formation. It is likely that protein G was deeply embedded in the Ag shell and remained on the Au/Ag core−shell surface even after boiling. Antibodies from various sources were also stably immobilized onto Au/Ag@PG (SI Figure S6).

Antigen binding ability of the antibody-conjugated Au/Ag core−shell NPs (Au/Ag@PG-AB) was investigated through in vitro binding experiments (Figure 4). Varying concentrations of
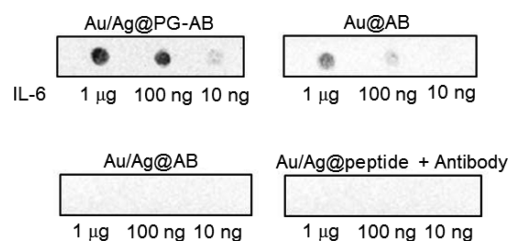

Figure 4. In vitro binding experiments. A series of diluted IL-6 solutions were spotted on an NC membrane. Antibody-conjugated Au/Ag core−shell NPs via embedded protein G (Au/Ag@PG-AB), antibody adsorbed AuNPs (Au@AB), silver deposited Au@AB NPs (Au/Ag@AB), and only peptide covered Au/Ag core−shell NPs (Au/Ag@peptide) with added antibody were applied to the IL-6 spotted membrane.

antigen (IL-6) were spotted on an NC membrane. Differently prepared IL-6 antibody-conjugated NPs were treated to the surface-bound IL-6 spots, and particle targeting was again directly measured by naked-eye detection without any amplification processes. Interestingly, surface IL-6 detection by Au/Ag@PG-AB was nearly 10-fold more sensitive than that by AuNPs of similar size (20 nm) with randomly adsorbed antibodies (Au@AB). The bright color of Ag shells and optimal antibody orientations on protein G-embedded Au/Ag core−shell NPs likely contribute to this highly enhanced surface antigen detection. Protein G-omitted Au/Ag NPs (Au/Ag@peptide, negative control) show no detectable antigen targeting signals. Antibody-bound Au/Ag core−shell NPs were also prepared by Ag deposition on antibody-adsorbed Au@AB without protein G and peptide linkers (Au/Ag@AB). The resulting Au/Ag@AB was unable to bind to the IL-6 spots (Figure 4). It is likely that functional Au/Ag@AB NPs were aggregated during binding experiments. In addition, irregular Ag shells (SI Figure S2) may bury many antigen binding sites of antibodies. These antigen binding data indicate that a uniform

Table 1. Dynamic Light Scattering (DLS) Measurement for Fabricated Nanoparticles

	AuNPs	Au@PG	Au/Ag@PG	Au@PG-AB	Au/Ag@PG-AB	Au@AB
DLS, avg (nm)	14.1 ± 3.1	28.3 ± 8.5	29.1 ± 7.0	33.4 ± 7.7	34.5 ± 8.4	38.3 ± 19.8

peptide/protein G layer on AuNPs is also critical for aqueous stability of Au/Ag core−shell NPs. Improved antigen detection by Au/Ag@PG-AB was also observed with the PSA antigen (SI Figure S7).

Finally, silver surfaces of the protein G-embedded Au/Ag core−shell NPs were investigated as surface-enhanced Raman scattering (SERS) active substrates. Protein G-conjugated AuNPs (Au@PG) and protein G-embedded Au/Ag core−shells (Au/Ag@PG) were addressed to surface-bound antibodies on a gold chip. Unbound NPs were washed from the surface, and therefore a particle layer can be formed on the gold surface. Rhodamine B isothiocyanate (RhB) solution was evenly applied to the surface, and the surface was air-dried before SERS measurement. Significantly enhanced SERS signals were observed only on the Au/Ag@PG surface without any distinct RhB SERS signals on the Au@PG surface (SI Figure S8).[31] A layer of the bio-functionalized Au/Ag core−shell NPs provided highly active Raman hot spots for randomly treated RhB molecules.

To develop more specific (and reproducible) SERS nanostructures from the protein G-embedded Au/Ag core sells, we next fabricated an Au/Ag@PG SERS probe by introducing Raman dye molecules uniformly on the Ag shell surface (Figure 5a). TAMRA was linked to the C-terminal of the Peptide Linker, and this dye-labeled peptide was additionally used for protein G-embedded Au/Ag core−shell NP formation. The resulting Au/Ag@PG-TAMRA features evenly displayed protein G and TAMRA dyes on the Ag shell surface (Figure 5a). TAMRA-conjugated NPs were again addressed to surface-bound antibodies on a gold chip. As shown in Figure 5b, greatly enhanced (TAMRA-specific) Raman signals were observed from surface-bound Au/Ag@PG-TAMRA. TAMRA SERS signals on the Ag shells were more than 100-fold higher than those obtained from AuNP-bound TMARA (Au@PG-TAMRA).

4. CONCLUSION

In the present study, we fabricated protein G-embedded Au/Ag core−shell nanoparticles that allow simple but optimally oriented antibody conjugation and provide strong optical characteristics of Ag surfaces. A linearly structured peptide linker was introduced for uniform peptide/protein layer formation on AuNP surfaces and successful protein-embedded Ag shell deposition. This work presents the first example of controlled embedment of a functional protein in Ag nanostructures. Stably embedded protein G on Au/Ag structures offers a highly effective immuno-silver staining strategy. Protein-functionalized SERS probes could also be consistently prepared by using synthetic Peptide Linker. The suggested protein embedment strategy can be applied with many other recombinant proteins with various functionalities. In addition, facile fabrication processes that require direct protein self-assemblies, commercial chemical deposition, and centrifugal purifications will facilitate use of silver nanostructures in biomedical and bioanalytical applications.

■ ASSOCIATED CONTENT

Ⓢ Supporting Information

Additional figures for protein sequences, TEM images, DLS data, binding blots, and Raman spectra as described in the text. This material is available free of charge via the Internet at http://pubs.acs.org.

■ AUTHOR INFORMATION

Corresponding Author
*Email: ywjung@kaist.ac.kr.
Notes
The authors declare no competing financial interest.

■ ACKNOWLEDGMENTS

■ REFERENCES

(1) Cobley, C. M.; Chen, J.; Cho, E. C.; Wang, L. V.; Xia, Y. Gold Nanostructures: A Class of Multifunctional Materials for Biomedical Applications. *Chem. Soc. Rev.* **2011**, *40*, 44−56.
(2) Cao, Y. C.; Jin, R.; Mirkin, C. A. Nanoparticles with Raman Spectroscopic Fingerprints for DNA and RNA Detection. *Science* **2002**, *297*, 1536−1540.
(3) Giljohann, D. A.; Seferos, D. S.; Daniel, W. L.; Massich, M. D.; Patel, P. C.; Mirkin, C. A. Gold Nanoparticles for Biology and Medicine. *Angew. Chem. Int. Ed. Engl.* **2010**, *49*, 3280−3294.
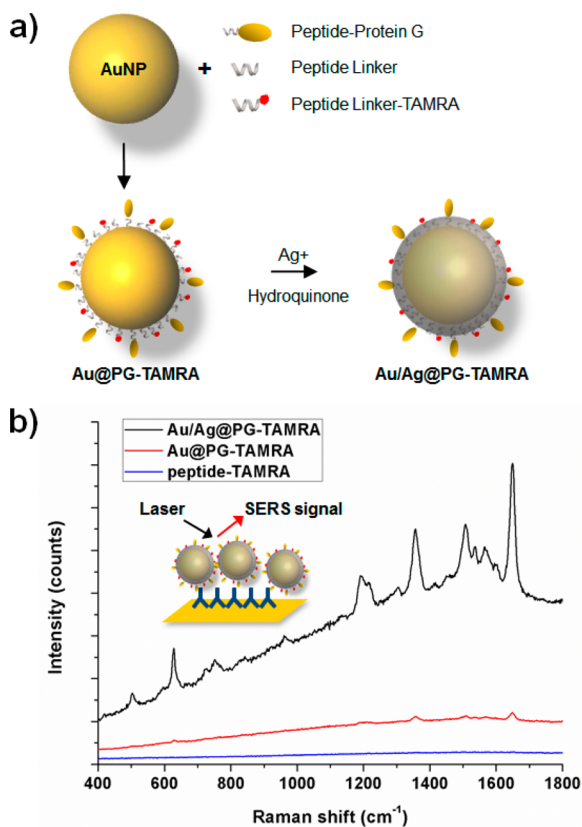

Figure 5. SERS measurement of TAMRA modified NPs. (a) Schematic representations of the preparation of Au/Ag core−shell NPs with embedded protein G and peptide-linked TAMRA (Au/Ag@PG-TAMRA). (b) Raman spectra of surface bound Au/Ag@PG-TAMRA (black), Au@PG-TAMRA (red), and only peptide-TAMRA (blue).

(4) Zhou, Y. G.; Rees, N. V.; Compton, R. G. The Electrochemical Detection and Characterization of Silver Nanoparticles in Aqueous Solution. *Angew. Chem. Int. Ed. Engl.* **2011**, *50*, 4219−4221.

(5) Zhu, Z.; Meng, H.; Liu, W.; Liu, X.; Gong, J.; Qiu, X.; Jiang, L.; Wang, D.; Tang, Z. Superstructures and SERS Properties of Gold Nanocrystals with Different Shapes. *Angew. Chem. Int. Ed. Engl.* **2011**, *50*, 1593−1596.

(6) Zhu, Z.; Liu, W.; Li, Z.; Han, B.; Zhou, Y.; Gao, Y.; Tang, Z. Manipulation of Collective Optical Activity in One-Dimensional Plasmonic Assembly. *ACS Nano* **2012**, *6*, 2326−2332.

(7) Arvizo, R.; Bhattacharya, R.; Mukherjee, P. Gold Nanoparticles: Opportunities and Challenges in Nanomedicine. *Expert Opin. Drug Delivery* **2010**, *7*, 753−763.

(8) Rosi, N. L.; Giljohann, D. A.; Thaxton, C. S.; Lytton-Jean, A. K.; Han, M. S.; Mirkin, C. A. Oligonucleotide-Modified Gold Nanoparticles for Intracellular Gene Regulation. *Science* **2006**, *312*, 1027−1030.

(9) Ananth, A. N.; Daniel, S. C.; Sironmani, T. A.; Umapathi, S. PVA and BSA Stabilized Silver Nanoparticles Based Surface-Enhanced Plasmon Resonance Probes for Protein Detection. *Colloids Surf., B* **2011**, *85*, 138−144.

(10) Li, Z.; Cheng, E.; Huang, W.; Zhang, T.; Yang, Z.; Liu, D.; Tang, Z. Improving the Yield of Mono-DNA-Functionalized Gold Nanoparticles through Dual Steric Hindrance. *J. Am. Chem. Soc.* **2011**, *133*, 15284−15287.

(11) Kelly, K. L.; Coronado, E.; Zhao, L. L.; Schatz, G. C. The Optical Properties of Metal Nanoparticles: The Influence of Size, Shape, and Dielectric Environment. *J. Phys. Chem. B* **2003**, *107*, 668−677.

(12) Lu, Y.; Mei, Y.; Drechsler, M.; Ballauff, M. Thermosensitive Core/Shell Particles as Carriers for Ag Nanoparticles: Modulating the Catalytic Activity by a Phase Transition in Networks. *Angew. Chem. Int. Ed. Engl.* **2006**, *45*, 813−816.

(13) Chu, X.; Xiang, Z. F.; Fu, X.; Wang, S. P.; Shen, G. L.; Yu, R. Q. Silver-Enhanced Colloidal Gold Metalloimmunoassay for Schistosoma Japonicum Antibody Detection. *J. Immunol. Methods* **2005**, *301*, 77−88.

(14) Oliver, C. Use of Immunogold with Silver Enhancement. *Methods Mol. Biol.* **2010**, *588*, 311−316.

(15) Taton, T. A.; Mirkin, C. A.; Letsinger, R. L. Scanometric DNA Array Detection with Nanoparticle Probes. *Science* **2000**, *289*, 1757−1760.

(16) Bharill, S.; Chen, C.; Stevens, B.; Kaur, J.; Smilansky, Z.; Mandecki, W.; Gryczynski, I.; Gryczynski, Z.; Cooperman, B. S.; Goldman, Y. E. Enhancement of Single-Molecule Fluorescence Signals by Colloidal Silver Nanoparticles in Studies of Protein Translation. *ACS Nano* **2011**, *5*, 399−407.

(17) Kneipp, K.; Kneipp, H.; Kneipp, J. Surface-Enhanced Raman Scattering in Local Optical Fields of Silver and Gold Nanoaggregatesfrom Single-Molecule Raman Spectroscopy to Ultrasensitive Probing in Live Cells. *Acc. Chem. Res.* **2006**, *39*, 443−450.

(18) Lim, D. K.; Jeon, K. S.; Kim, H. M.; Nam, J. M.; Suh, Y. D. Nanogap-Engineerable Raman-Active Nanodumbbells for Single-Molecule Detection. *Nat. Mater.* **2010**, *9*, 60−67.

(19) Lee, H.; Lee, J. H.; Jin, S. M.; Suh, Y. D.; Nam, J. M. Single-Molecule and Single-Particle-Based Correlation Studies between Localized Surface Plasmons of Dimeric Nanostructures with ∼1 nm Gap and Surface-Enhanced Raman Scattering. *Nano Lett.* **2013**, *13*, 6113−6121.

(20) Vu, T. K. T.; Nguyen, Q. D.; Nguyen, T. D.; Trinh, T. H. Preparation of Metal Nanoparticles for Surface Enhanced Raman Scattering by Laser Ablation Method. *Adv. Nat. Sci. Nanosci. Nanotechnol.* **2012**, *3*, 025016.

(21) Hubenthal, F.; Hendrich, C.; Träger, F. Damping of the Localized Surface Plasmon Polariton Resonance of Gold Nanoparticles. *Applied Physics B* **2010**, *100*, 225−230.

(22) Szymanski, M. S.; Porter, R. A. Preparation and Quality Control of Silver Nanoparticle/Antibody Conjugate for Use in Electrochemical Immunoassays. *J. Immunol. Methods* **2013**, *387*, 262−269.

(23) Bahadur, N. M.; Furusawa, T.; Sato, M.; Kurayama, F.; Siddiquey, I. A.; Suzuki, N. Fast and Facile Synthesis of Silica Coated Silver Nanoparticles by Microwave Irradiation. *J. Colloid. Interface Sci.* **2011**, *355*, 312−320.

(24) Skewis, L. R.; Reinhard, B. M. Control of Colloid Surface Chemistry through Matrix Confinement: Facile Preparation of Stable Antibody Functionalized Silver Nanoparticles. *ACS Appl. Mater. Interfaces* **2010**, *2*, 35−40.

(25) Lee, J. S.; Lytton-Jean, A. K.; Hurst, S. J.; Mirkin, C. A. Silver Nanoparticle-Oligonucleotide Conjugates Based on DNA with Triple Cyclic Disulfide Moieties. *Nano Lett.* **2007**, *7*, 2112−2115.

(26) Lim, D. K.; Kim, I. J.; Nam, J. M. DNA-Embedded Au/Ag Core/Shell Nanoparticles. *Chem. Commun.* **2008**, *42*, 5312−5314.

(27) Jung, Y.; Lee, J. M.; Jung, H.; Chung, B. H. Self-Directed and Self-Oriented Immobilization of Antibody by Protein G-DNA Conjugate. *Anal. Chem.* **2007**, *79*, 6534−6541.

(28) Jung, Y.; Jeong, J. Y.; Chung, B. H. Recent Advances in Immobilization Methods of Antibodies on Solid Supports. *Analyst* **2008**, *133*, 697−701.

(29) Arai, R.; Ueda, H.; Kitayama, A.; Kamiya, N.; Nagamune, T. Design of the Linkers Which Effectively Separate Domains of a Bifunctional Fusion Protein. *Protein Eng.* **2001**, *14*, 529−532.

(30) Bhushan, S.; Gartmann, M.; Halic, M.; Armache, J. P.; Jarasch, A.; Mielke, T.; Berninghausen, O.; Wilson, D. N.; Beckmann, R. A-Helical Nascent Polypeptide Chains Visualized within Distinct Regions of the Ribosomal Exit Tunnel. *Nat. Struct. Mol. Biol.* **2010**, *17*, 313−317.

(31) Li, D.; Li, D. W.; Li, Y.; Fossey, J. S.; Long, Y. T. Cyclic Electroplating and Stripping of Silver on Au@SiO$_2$ Core/Shell Nanoparticles for Sensitive and Recyclable Substrate of Surface-Enhanced Raman Scattering. *J. Mater. Chem.* **2010**, *20*, 3688−3693.